Analysis of unsteady MHD Copper-Water nanofluid flow and heat transfer between two parallel surfaces under suction and injection

W. Abbas[1], Michael Haleam[2], Ahmed M. Megahed[3], Ramadan Awadalla[2]
[1]Basic and Applied Sciences Department, College of Engineering and Technology, Arab Academy for Science and Technology, Cairo, Egypt.
[2]Physics and Engineering Mathematics Department, Faculty of Engineering- Elmattaria, Helwan University, Cairo, Egypt.
[3] Department of Mathematics, Faculty of Science, Benha University, Benha, Egypt.

Abstract

Unsteady Magnetohydrodynamic (MHD) flow of nanofluid between two infinite parallel porous plates was investigated with considering Heat transfer and Hall Effect under constant pressure gradient. In this study, Copper as nanoparticle with water as its base fluid has been considered. The governing partial differential equations subjected to appropriate boundary conditions were derived and solved semi-analytically with homotopy perturbation method (HPM). The effects of physical parameters are graphically presented for varies values such as, the nanofluid volume fraction, Hartmann number and Reynolds number on non-dimensional velocity and temperature profile are considered. The results show that, increase in nanoparticle volume fraction $\emptyset$ increase the amount of heat transfer to the nanofluid and hence its temperature increases.

Keywords: Unsteady flow, Nanofluid, Couette flow, MHD, Homotopy perturbation method.

1. Introduction

Due to the numerous uses of nanofluid in science, engineering, and technology, challenges with its flow in tubes or channels have attracted increased attention in recent years. Examples include refrigeration, solar water heating, cooling of nuclear systems, and engine cooling [1]. The term “Nanofluids” is defined as a mixture of nanoparticles (nominally 1-100 nm in size) suspended in a base fluid [2], this term was introduced by Choi [3] in 1995. Since then, many research investigated nanofluids for heat transfer improvement in different thermal applications. Xie et al. [4], investigated the thermal conductivity behavior of SiC dilute nanoparticle-fluid mixtures with spherical and cylindrical shapes of SiC nanoparticles. Jang and Choi [5] studied the effects of the ratio of the thermal conductivity of nanoparticles to that of a base fluid, volume fraction, nanoparticle size, and temperature on the effective thermal conductivity of nanofluids. The dependence of size of nanoparticles and temperature on the effective thermal conductivity of nanofluids was proposed by Shukla, and Dhir [6] based on the theory of Brownian motion of nanoparticles in a fluid. Abu-Nada [7] evaluated the role of both viscosity and thermal conductivity, derived from experimental data, on heat transfer in natural convection. The convective heat transfer characteristics of silver–water nanofluid under laminar and turbulent flow conditions were experimentally measured by Gogson et al. [8]. Chandraprabu et al. [9] compared the heat transfer performance of the nanofluids Al2O3/water and CuO/water in the condensing unit of air conditioner for various flow rates. The experimental results of nanofluids are compared with water for various volume fractions and showed that the heat transfer enhancement is caused by suspending nanoparticles and becomes more pronounced with the increase of the particle volume concentration.

Recently, researchers have considerable interest in the study of fully developed nanofluids flow between parallel plates. This is because of its significant importance in many applications such as power generation systems, heat exchangers, car engines cooling and electronic devices. Peyghambarzadeh et al. [10] experimentally investigated the heat transfer of forced convection in AL2O3/Water nanofluid with different concentrations to that of pure water in an automobile radiator and found that . Leong et al. [11] analytically investigated the performance of nanofluids as the heat transfer fluid in a thermosyphon heat recovery exchanger. The influence of Reynolds number and solid volume fraction on forced convection boundary layer flow inside the direct absorption solar collector with Copper/water nanofluid was investigated by Pravin et al. [12]. Khaleduzzaman et al. [13] experimentally analyzed the energy, exergy, and friction factor of a rectangular minichannel heat sink using AL2O3/Water nanofluid with different volume fractions. Abbas et al. study [14] examined how Soret and Dufour's theories affected the mass transfer and mixed convection heat of Peristaltic Flow of Casson Fluid Through NonDarcy Porous Medium Inside Vertical Channel. Hsiao [15] investigated the heat and mass transfer of nanofluid flow across a stretching sheet that forms a slip boundary.. Williamson nanofluid flow across a stretching sheet was studied numerically by Khan et al. [16] in relation to an angled Lorentz force and fluctuating viscosity. Pal and Roy [17] investigated the complementary effects of non-uniform heat source/sink and nonlinear thermal radiation in the boundary layer flow. Considering variables, they examined the phenomenon of heat transfer over a stretching surface of a Casson nanofluid. Abbas and Magdy [18] examined the heat transmission and motion of an unstable nanofluid past a rotating plate with Brownian motion, as well as the effects of thermophoresis diffusion. The three-dimensional continuous thin-film flow across a stretching surface of tangent hyperbolic fluid with nonlinear Entropy formation was investigated by Ibrahim and Gizewu [19] using mixed convection flow. An analytical study by Loganathan et al. [20] examined the effects of a heated porous Riga plate that absorbs heat in conjunction with viscoelastic nanofluidic flow and Cattaneo-Christov dual flow. Shao et al.'s research [21] examined the significance of visco-elastic Motion that conducts electricity and materials that alter over time outperform a capsule's surface due to gravity.

Magnetohydrodynamic (MHD) flow with heat transfer has received considerable attention in the recent years because of their wide variety of applications such as MHD generator, cooling of nuclear reactor, electronic package, MHD pump, microelectronic devices, plasma physics, and solar technology [22], [23]. The magneto convection flow of two immiscible fluids through a vertical channel with heat generation and absorption were analytically and numerically investigated by Umavathi et al. [24]. Kandaswamy et al. [25] numerically investigated the Magnetoconvection of an electrically conducting fluid in a square cavity with partially thermally active vertical walls. unsteady Magnetohydrodynamic flow with heat and mass transfer near the stagnation point of a three-dimensional porous body in the presence of heat source/sink and chemical reaction effect has been numerically studied by Chamkha and Ahmed [26]. Nemati et al. [27] studied the effect of CuO nanoparticles on natural convection with magnetohydrodynamic flow in a square cavity. Couette MHD flow with heat transfer through a porous medium between two parallel plates was investigated by abdeen et al. [28] considering the Hall current and variable properties. The MHD unstable nanofluid flow across a stretching sheet was accompanied by the effects of heat radiation, injection and suction, and multiple slip on mass and heat transfer. The magnetic field's alignment's stretching effect Williamson used convective boundary conditions on a surface for his numerical investigation of nanofluid flow. from Indraprastha et al. [29]. Megahed conducted an examination of the non-linear MHD of a porous medium with an embedded stretched sheet under a convective boundary condition of Newtonian Maxwell fluid flow [30]. Biswal et al. [31] presented the 2 MHD free convective stagnation-point flow. Moreover, the wide variety of non-Newtonian fluids makes it impractical to rely on a single fundamental equation to fully describe the behavior displayed by each of these fluid kinds ([32])-([33]). Among the different kinds of non-Newtonian fluid models, the tangent hyperbolic fluid model is one of the most important and prominent ones. The flow properties of tangent hyperbolic fluid in a boundary layer created by a stretched sheet were examined in the first formulation of the tangent hyperbolic fluid model. The model then describes a situation in which an increase in the shear effect causes the fluid's effective viscosity to decrease. Also, other recent interesting research studied of non-Newtonian fluid by referring to the cited citations ([34])-([38]).

The aim of the present study is to investigate the effect of nanoparticles on the unsteady magnetohydrodynamic flow between two infinite parallel porous plates with considering Heat transfer and Hall Effect under constant pressure gradient. Analysis is performed for copper nanoparticles by considering water as a base fluid. The resulting non-linear system has been semi-analytically with homotopy perturbation technique.

2. Problem discerption and mathematical formulation

We consider an unsteady nanofluid flow between two parallel horizontal porous plates, as shown in Figure 1. The boundary plates are infinite in the x- and z- directions and located at y=±h from the origin. The lower plate is stationary while the upper plate is moving with constant velocity u_0 in the x-direction. A uniform suction from above and injection from below are applied and the y component of the flow velocity is assumed constant and denoted as v_0. The lower and upper plates are maintained at constant temperatures T_1 and T_2 respectively with $T_2 > T_1$. The nanofluid is assumed to be Newtonian, incompressible, and fully developed flow driven by a constant pressure gradient in the x-direction. The flow is under the influence of a uniform magnetic field with constant flux density B_0 applied in the y-direction. Due to the Hall effect a velocity component in z-direction w is developed.

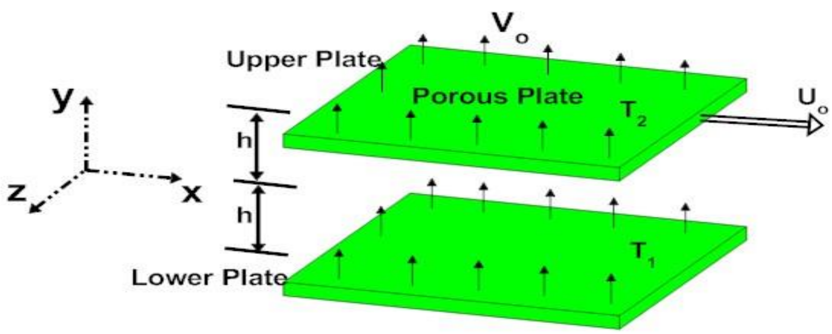

Figure 1: Schematic of problem

Additionally, we express the magnetic field induced Lorentz force per unit volume as [28]:

$$\vec{F} = \vec{J} \times \vec{B} \tag{1}$$

Where, $\vec{B}$ is the induced magnetic vector, and $\vec{J}$ is the electric current density vector which can be obtained by generalized Ohm's law including Hall current as [39]:

$$\vec{J} = \sigma[\vec{E} + \vec{v} \times \vec{B} - \beta\left(\vec{J} \times \vec{B}\right)] \tag{2}$$

Where, σ is the electric conductivity of the fluid, $\vec{v}$ is the velocity vector, $\vec{v}(y,t) = u(y,t)\vec{i} + v_0\vec{j} + w(y,t)\vec{k}$, $\vec{E}$ is the intensity vector of the electric field, and β is the Hall factor. By neglecting polarization effect, we get the electric field vector equal zero ($\vec{E}$=0). Equation (1) may be solved in $\vec{J}$ to yield:

$$\vec{F} = \frac{\sigma B_0}{1+m^2}(mu - w)\vec{i} + \frac{\sigma B_0}{1+m^2}(u + mw)\vec{k} \quad (3)$$

Where, m is the Hall parameter, $m = \beta\, \sigma B_0$.

2.1 Equation formulation

Under these assumptions, the continuity, momentum and energy equations are written as follows [28, 39]:

Continuity equation:

$$\frac{\partial v}{\partial y} = 0 \quad (4)$$

Momentum equation in x-direction:

$$\rho_{nf}\frac{\partial u}{\partial t} + \rho_{nf} v_0 \frac{\partial u}{\partial y} = -\frac{\partial P}{\partial x} + \mu_{nf}\frac{\partial^2 u}{\partial y^2} - \frac{\sigma_{nf} {B_0}^2}{1+m^2}(w + mu) \quad (5)$$

Momentum equation in z-direction:

$$\rho_{nf}\frac{\partial w}{\partial t} + \rho_{nf} v_0 \frac{\partial w}{\partial y} = \mu_{nf}\frac{\partial^2 w}{\partial y^2} - \frac{\sigma_{nf} {B_0}^2}{1+m^2}(w - mu) \quad (6)$$

Energy equation:

$$(\rho c_P)_{nf}\frac{\partial T}{\partial t} + (\rho c_P)_{nf} v_0 \frac{\partial T}{\partial y} = K_{nf}\frac{\partial^2 T}{\partial y^2} + \mu\left[\left(\frac{\partial u}{\partial y}\right)^2 + \left(\frac{\partial w}{\partial y}\right)^2\right] + \frac{\sigma_{nf} {B_0}^2}{1+m^2}(u^2 + w^2) \quad (7)$$

Where, u and w are the fluid velocity components in the x and z directions respectively. ρ_{nf} is the nanofluid density, P represent the pressure, μ_{nf} is the nanofluid viscosity, T denotes the temperature, σ_{nf} is the electric conductivity of the nanofluid, B_0 is the magnetic field density, and m is the hall parameter ($m = \sigma_{nf}\beta B_0$) where β is the hall factor [39].

2.2 Initial and boundary conditions

In the present investigation, we assumed the initial and boundary conditions used in solving the problem are:

$$t \le 0 \quad u = 0; \quad w = 0; \quad T = 0 \quad (8a)$$

$$t > 0 \quad u = 0; \quad w = 0; \quad T = T_1; \quad y = -h \quad (8b)$$

$$t > 0 \quad u = u_0; \quad w = 0; \quad T = T_2; \quad y = h \quad (8c)$$

2.3 Nanoparticle thermo-physical properties

In the current study, the thermo-physical properties of the nanofluid were determined using the following relations [40, 41]:

The density (ρ_{nf}) and heat capacity ($(\rho c_P)_{nf}$) of the nanofluid, and the electric conductivity (σ_{nf}) are defined as:

$$\rho_{nf} = (1-\emptyset)\rho_f + \emptyset\rho_p \tag{9}$$

$$(\rho c_P)_{nf} = (1-\emptyset)(\rho c_P)_f + \emptyset(\rho c_P)_p \tag{10}$$

$$\sigma_{nf} = (1-\emptyset)\sigma_f + \emptyset\sigma_p \tag{11}$$

According to Brinkman model the viscosity (μ_{nf}) of nanofluid is given as:

$$\mu_{nf} = \frac{\mu_f}{(1-\emptyset)^{2.5}} \tag{12}$$

The thermal conductivity (k_{nf}) is calculated using the Maxell model as:

$$k_{nf} = \frac{k_p + 2k_f - 2\emptyset(k_f - k_p)}{k_p + 2k_f + \emptyset(k_f - k_p)} k_f \tag{13}$$

Where, $\emptyset$ is the volume fraction of nanofluid and the subscripts f, nf, and p denotes base fluid, nanofluid and solid particle respectively.

2.4 Dimensionless parameters

Introducing these non-dimensional parameters to the above equations

$$x^* = \frac{x}{h}, \quad y^* = \frac{y}{h}, \quad z^* = \frac{z}{h}, \quad t^* = \frac{tu_0}{h}, \quad u^* = \frac{u}{u_0}, \quad w^* = \frac{w}{u_0},$$
$$\rho^* = \frac{\rho}{\rho_f {u_0}^2}, \quad T^* = \frac{T - T_1}{T_2 - T_1}$$

The continuity, momentum and energy equations can be written in non-dimensional form as follows:

Continuity equation:

$$\frac{\partial v^*}{\partial y^*} = 0 \tag{14}$$

Momentum equation in x-direction:

$$\frac{\partial u^*}{\partial t^*} + S\frac{\partial u^*}{\partial y^*} = -\frac{\partial P^*}{\partial x^*} + \frac{\rho_f}{Re(1-\emptyset)^{2.5}\rho_{nf}}\frac{\partial^2 u^*}{\partial {y^*}^2} - \frac{Ha^2\rho_f}{Re(1+m^2)\rho_{nf}}(u^* + mw^*) \tag{15}$$

Momentum equation in z-direction:

$$\frac{\partial w^*}{\partial t^*}+S\frac{\partial w^*}{\partial y^*}=\frac{\rho_f}{Re(1-\emptyset)^{2.5}\rho_{nf}}\frac{\partial^2 w^*}{\partial y^{*2}}-\frac{Ha^2\rho_f}{Re(1+m^2)\rho_{nf}}(w^*-mu^*) \quad (16)$$

Energy equation:

$$\frac{\partial T^*}{\partial t^*}+S\frac{\partial T^*}{\partial y^*}=$$
$$\frac{K_{nf}\rho_f c_{p_f}}{Re(\rho c_P)_{nf}PrK_f}\frac{\partial^2 T^*}{\partial y^{*2}}+\frac{Ec(\rho c_P)_f}{Re(1-\emptyset)^{2.5}(\rho c_P)_{nf}}\left[\left(\frac{\partial u^*}{\partial y^*}\right)^2+\left(\frac{\partial w^*}{\partial y^*}\right)^2\right]+\frac{Ha^2Ec(\rho c_P)_f}{Re(1+m^2)(\rho c_P)_{nf}}\left(u^{*2}+w^{*2}\right) \quad (17)$$

In the above equations, $S=\frac{v_0}{u_0}$ is the suction parameter, $Re=\frac{\rho_f u_0 h}{\mu_f}$ is the Reynolds number, $Ha^2=\frac{\sigma_{nf}{B_0}^2h^2}{\mu_f}$ is the Hartmann number, $Pr=\frac{c_{p_f}\mu_f}{k_f}$ is the Prandtl number, and $Ec=\frac{{u_0}^2}{c_{p_f}(T_2-T_1)}$ is the Eckert number.

The corresponding non-dimensional initial and boundary conditions are:

$$t\leq 0 \quad u^*=0; \quad w^*=0; \quad T^*=0 \quad (18a)$$

$$t>0 \quad u^*=0; \quad w^*=0\,; \quad T^*=0; \quad y^*=-1 \quad (18b)$$

$$t>0 \quad u^*=1; \quad w^*=0; \quad T^*=0; \quad y^*=1 \quad (18c)$$

3 Method of Solutions

In order to solve the unsteady, coupled non-linear partial differential equations (15)-(17) under the initial and boundary conditions (18a)-(18c), can be solved analytically by using the method of homotopy perturbation. This method's process and primary definition have already been presented in several publications [42-44]. The solutions obtained are functions of the physical parameters of the problem. These solutions can be written as:

$$u_{(y,t)}=u_1(t)y+u_2(t)y^2+\cdots,$$

$$w_{(y,t)}=w_1(t)y+w_2(t)y^2+\cdots$$

$$T^*_{(y,t)}=T^*_1(t)y+T^*_2(t)y^2+\cdots$$

Where,

$$u_1=-(e^{-t\,w}-1)\,(y+1)$$

$$u_2 = \frac{e^{-tw}\left(\begin{array}{c} 6s - 6w + 12J_1 a - 2wy - 6se^{tw} - 6sy^2 + 6wy^2 + 2wy^3 \\ +6J_1 J_4 b + 6sy^2 e^{tw} + 12J_1 a y - 6GJ_1 e^{tw} - 6J_1 a e^{tw} - 6J_1 J_4 b \\ e^{tw} - 6J_1 J_4 b y^2 - 2J_1 J_4 b y^3 - 6J_1 a y e^{tw} + 6GJ_1 y^2 e^{tw} - 5J_1 J_4 b m \\ +2J_1 J_4 b y + 5J_1 J_4 b m e^{tw} - 2J_1 J_4 b y e^{tw} + 6J_1 J_4 b m y^2 - J_1 J_4 b m y^4 \\ +6J_1 J_4 b y^2 e^{tw} + 2J_1 J_4 b y^3 e^{tw} - \\ 6J_1 J_4 b m y^2 e^{tw} + J_1 J_4 b m y^4 e^{tw} \end{array}\right)}{12J_1 a}$$

$$w_1 = -(e^{-tw} - 1)(y - 1)(y + 1)$$

$$w_2 = \frac{e^{-tw}\left(\begin{array}{c} 5w + 4sy - 4sy^3 - 6wy^2 + wy^4 - 5J_1 J_4 b + 4sy^3 e^{tw} - 4sye^{tw} \\ +5J_1 J_4 b e^{tw} + 6J_1 J_4 b y^2 - J_1 J_4 b y^4 - 6J_1 J_4 b m \\ -2J_1 J_4 b m y + 6J_1 J_4 b m e^{tw} + 6J_1 J_4 b m y^2 \\ +2J_1 J_4 b m y^3 - 6J_1 J_4 b y^2 e^{tw} \\ +J_1 J_4 b y^4 e^{tw} - 6J_1 J_4 b m y^2 e^{tw} \\ -2J_1 J_4 b m y^3 e^{tw} + 2J_1 J_4 b m y e^{tw} \end{array}\right)}{12J_1 a}$$

$$T^*_1 = -(e^{-tw} - 1)(y - 1)(y + 1)$$

$$T^*_2 = \frac{\left(\begin{array}{c} 25\,Pr\,w\,e^{tw} + 20\,Pr\,s\,y\,e^{tw} - 20\,Pr\,s\,y\,e^{2tw} + 50\,Ec\,J_6\,Pr\,a - 20\,Pr\,s\,y^3 e^{tw} \\ +20\,Pr\,s\,y^3 e^{2tw} - 30\,Pr\,w\,y^2 e^{tw} + 5\,Pr\,w\,y^4 e^{tw} - 100\,Ec\,J_6\,Pr\,a\,e^{tw} \\ +50\,Ec\,J_6\,Pr\,a\,e^{2tw} - 30\,Ec\,J_6\,Pr\,a\,y^2 - 20\,Ec\,J_6\,Pr\,a\,y^4 + 57\,Ec\,J_4 J_6\,Pr\,b \\ +60\,Ec\,J_6\,Pr\,a\,y^2 e^{tw} - 30\,Ec\,J_6\,Pr\,a\,y^2 e^{2tw} + 40\,Ec\,J_6\,Pr\,a\,y^4 e^{tw} - 20\,Ec\,J_6\,Pr\,a\,y^4 e^{2tw} \\ +20\,Ec\,J_4 J_6\,Pr\,b\,y - 114\,Ec\,J_4 J_6\,Pr\,b\,e^{tw} \\ +57\,Ec\,J_4 J_6\,Pr\,b\,e^{2tw} - 60\,Ec\,J_4 J_6\,Pr\,b\,y^2 \\ -20\,Ec\,J_4 J_6\,Pr\,b\,y^3 + 5\,Ec\,J_4 J_6\,Pr\,b\,y^4 - 2\,Ec\,J_4 J_6\,Pr\,b\,y^6 - 40\,Ec\,J_4 J_6\,Pr\,b\,y\,e^{tw} \\ +20\,Ec\,J_4 J_6\,Pr\,b\,y\,e^{2tw} + 120\,Ec\,J_4 J_6\,Pr\,b\,y^2 e^{tw} + 40\,Ec\,J_4 J_6\,Pr\,b\,y^3 e^{tw} \\ -60\,Ec\,J_4 J_6\,Pr\,b\,y^2 e^{2tw} - 10\,Ec\,J_4 J_6\,Pr\,b\,y^4 e^{tw} - 20\,Ec\,J_4 J_6\,Pr\,b\,y^3 e^{2tw} \\ +5\,Ec\,J_4 J_6\,Pr\,b\,y^4 e^{2tw} + 4\,Ec\,J_4 J_6\,Pr\,b\,y^6 e^{tw} - 2\,Ec\,J_4 J_6\,Pr\,b\,y^6 e^{2tw} \end{array}\right)}{60J_6\,(J_5\,e^{2tw} - J_4\,Pr\,RR\,e^{2tw})}$$

4 Results and discussion

In the present study, copper (Cu) nanoparticles are considered with water as the base fluid. We have used data related to the thermos physical properties of the fluid and nanoparticles as listed in table 1 [18]. The value of the Prandtl number, Reynolds number, and Eckert number are assumed to be 1, 1,and 0.2, respectively. Also the volume fraction of nanoparticles is from 0 to 0.1 ($0 \leq \emptyset \leq 0.06$) in which $\emptyset = 0$ corresponds to the regular Newtonian fluid.

Table 1: The physical properties of nanofluids and base fluid

Properties	Fluid (water)	Copper (Cu)
Cp (j/kgK)	4179	385
ρ (kg/m³)	997.1	8933
K (W/Mk)	0.613	401

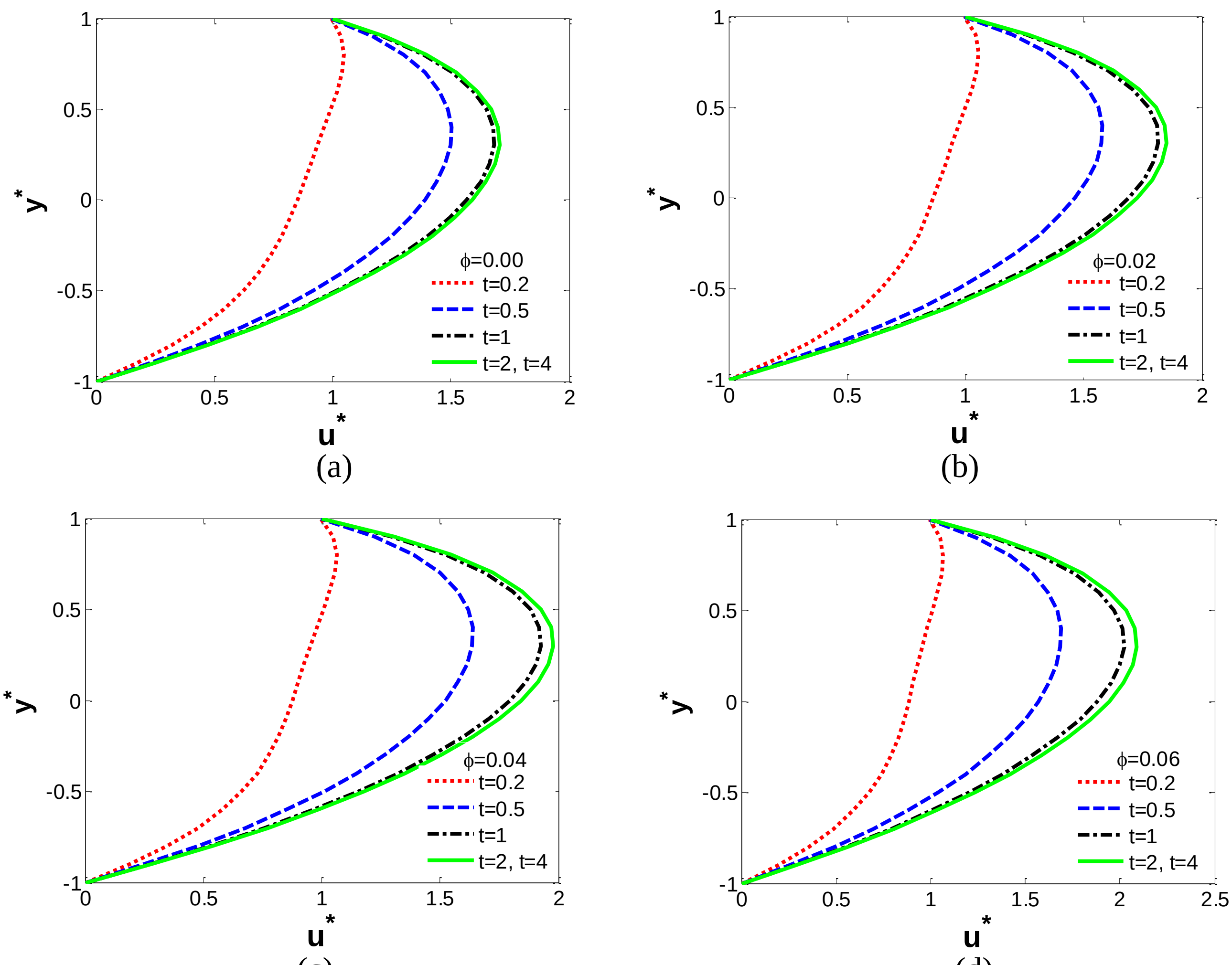

Figure 2: Time variation of the profile of u^* for different values of nanoparticle volume fraction $\emptyset$. (a) $\emptyset = 0$; (b) $\emptyset = 0.02$; (c) $\emptyset = 0.04$; (d) $\emptyset = 0.06$

Figures 2-4 present the time development of the profiles of the velocity and temperature distributions for various values of nanoparticle volume fractions $\emptyset$. Figures 2 and 3 displayed the effect of nanoparticle volume fractions $\emptyset$ on the dimensionless velocities components, it is observed that both velocity components u^* and w^* increase with the increase in the nanoparticle volume fraction $\emptyset$. As well, the increase of the volume fraction will increase the thermal conductivity of the nanofluid, this decreasing of fluid viscosity which increasing the moving of fluid.

The effect of nanoparticle volume fractions $\emptyset$ on temperature distribution T^* is shown in figure 4. It is observed that, increase in nanoparticle volume fraction $\emptyset$ increase the amount of heat transfer to the nanofluid and hence its temperature increases. This is due to the fact that as, increase of the volume fraction $\emptyset$ will increase the thermal conductivity of the nanofluid. This increases due to the increase of the surface area of the metallic nanoparticles, this lead to increases the nanolayer around the nanoparticles.

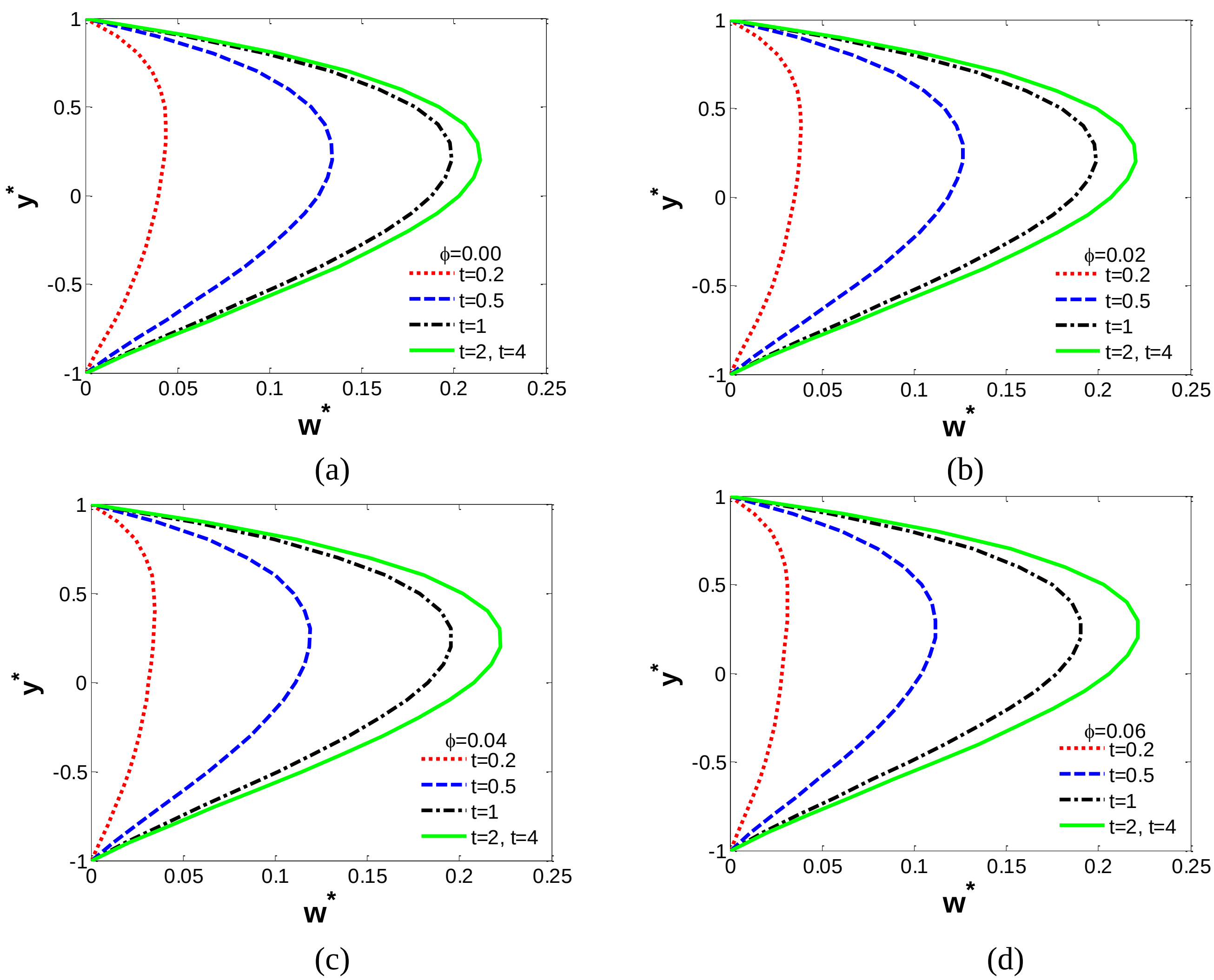

Figure 3: Time variation of the profile of w^* for different values of nanoparticle volume fraction $\emptyset$. (a) $\emptyset = 0$; (b) $\emptyset = 0.02$; (c) $\emptyset = 0.04$; (d) $\emptyset = 0.06$

Figure 5 present the effect of Hartmann parameter Ha on the velocity components (u^* and w^*) and temperature T^* at different values of nanoparticle volume fractions $\emptyset$. This figure illustrate that, with an increase of Hartmann number H_a, the velocity components u^* is reduced because the hydromagnetic drag force in equation (15) is proportional to the square of H_a, and remains with negative sign, as shown in figure 5(a). On the other hand, figure 5(b) indicates the velocity component w^* increases with a rise in Hartmann number Ha, this is because the effect of the hydromagnetic force in equation (16). Also, it is observed that, the temperature distribution T^* is increases with increasing Hartmann number H_a, as shown in figure 5(c). This is because increasing the contribution from the Joule dissipation term.

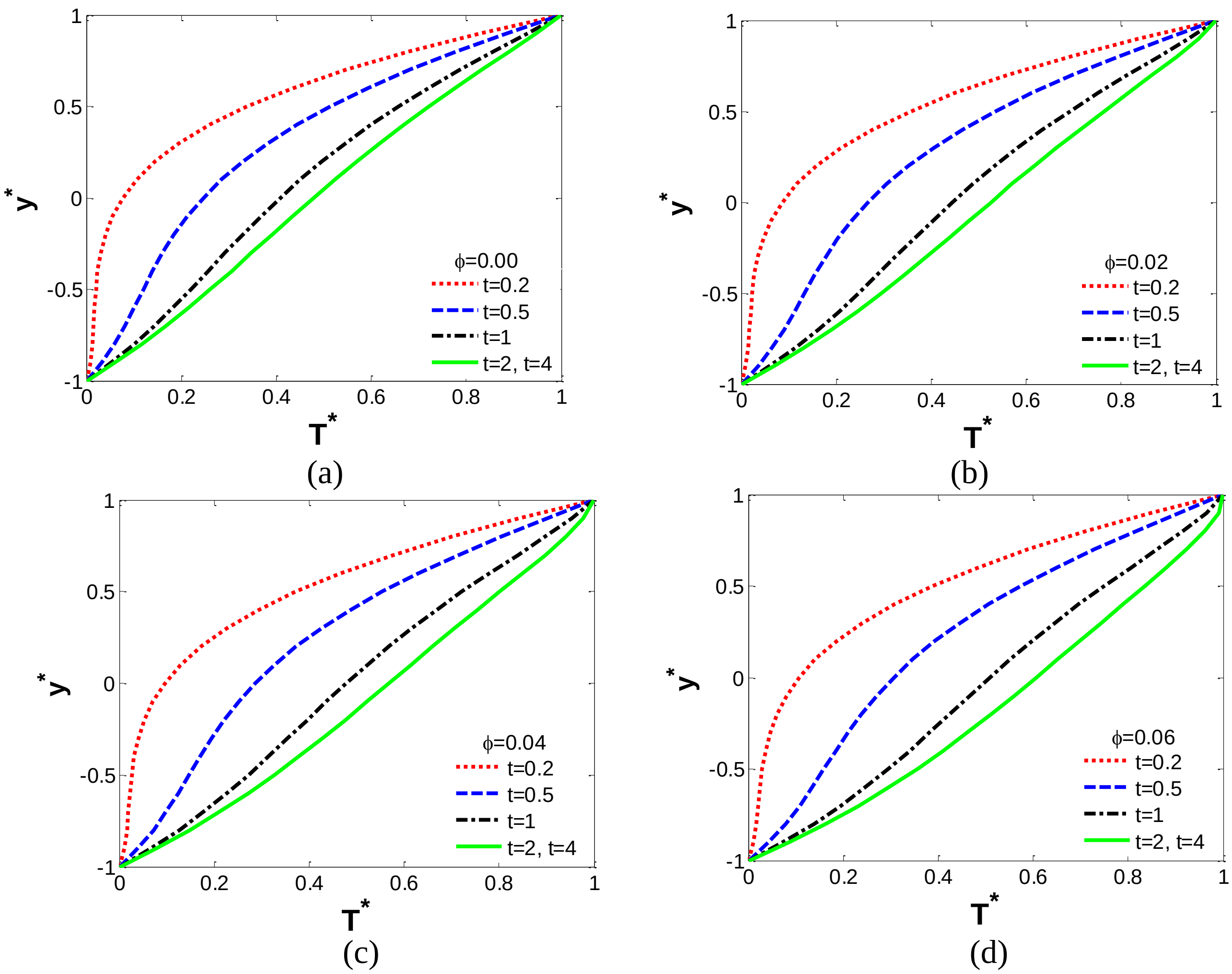

Figure 4: Time variation of the profile of T^* for diferent values of nanoparticle volume fraction $\emptyset$. (a) $\emptyset = 0$; (b) $\emptyset = 0.02$; (c) $\emptyset = 0.04$; (d) $\emptyset = 0.06$

Figure 6 illustrate the effect of Hall parameter m on the velocities component and temperature and for various values of nanoparticle volume fractions ∅. Figure 6(a) shows that, the velocity component u^* is increased with an increase in Hall parameter m, which can be attributed to the fact that the increase in m decreases the effective conductivity ($\frac{Ha^2 \rho_f}{Re(1+m^2)\rho_{nf}}$) and hence the magnetic damping. It is observed that, in figure 6(b) the velocity component w^* decreases with increasing the Hall parameter m, due to increasing its damping term $\frac{Ha^2 \rho_f}{Re(1+m^2)\rho_{nf}}(w^* - mu^*)$in equation (16). Also, it is found that, with increasing the Hall parameter m the fluid temperatures distribution T^* decreases. This is because decreasing the contribution from the Joule dissipation term, as shown in figure 6(c).

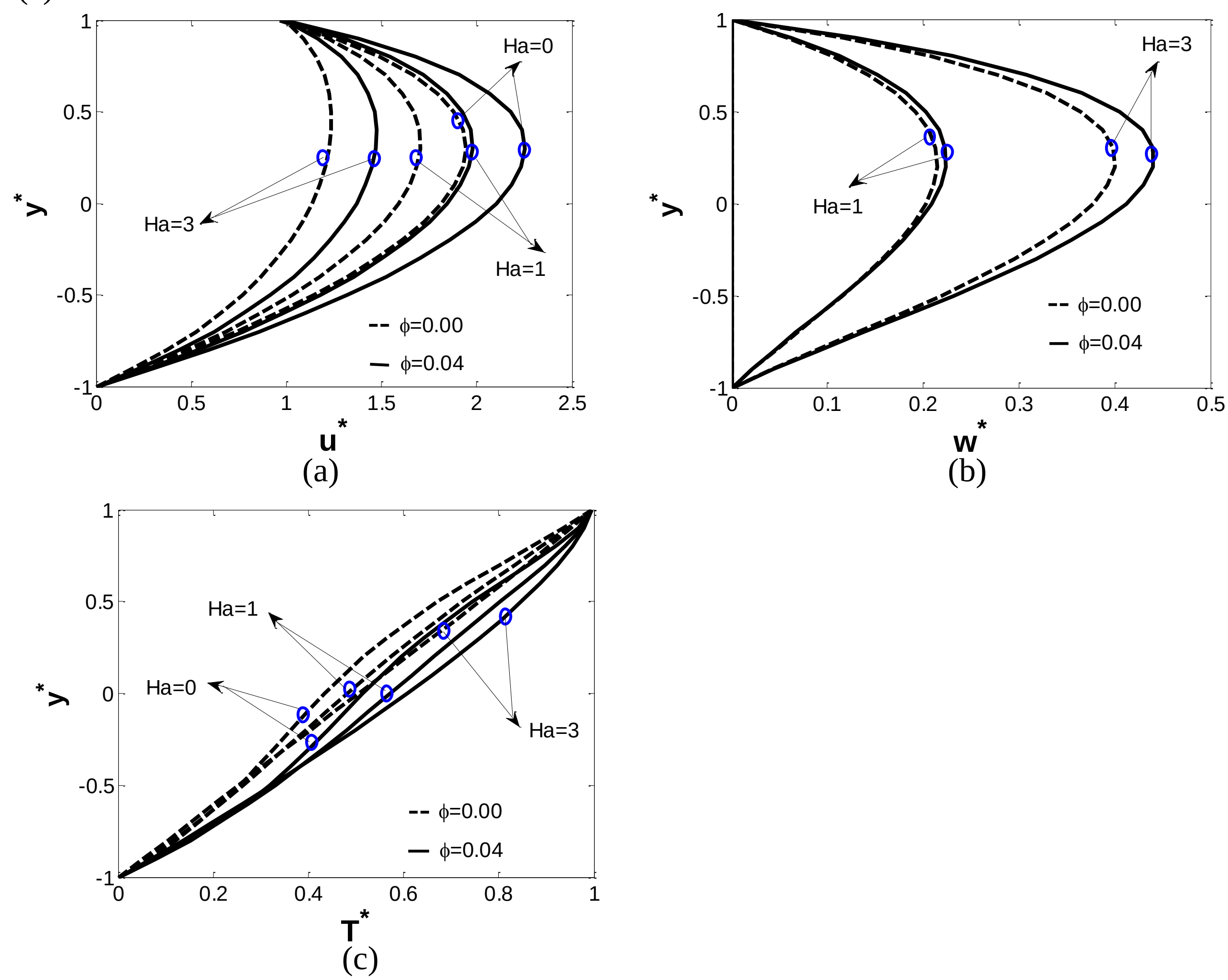

Figure 5: Effect of Hartmann parameter Ha on the velocities and temperature profiles at different values of nanoparticle volume fractions ∅.

(a) u^* Profile; (b) w^* Profile; (c) T^* Profile

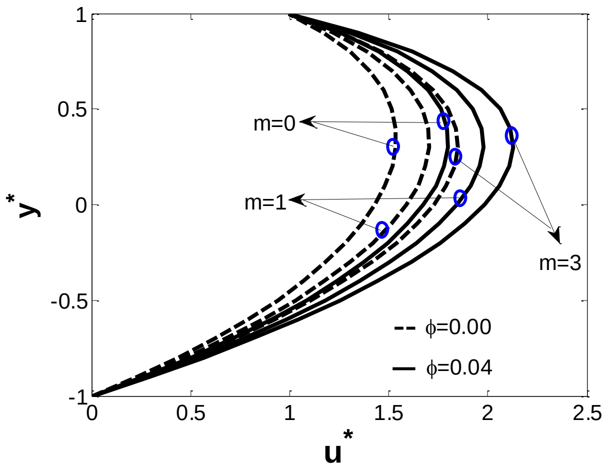

(a)

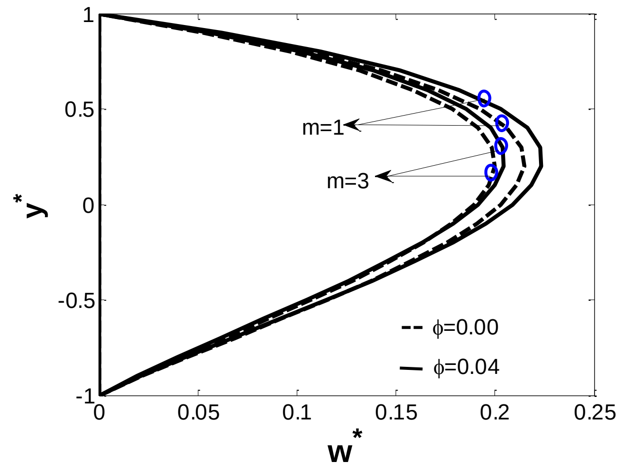

(b)

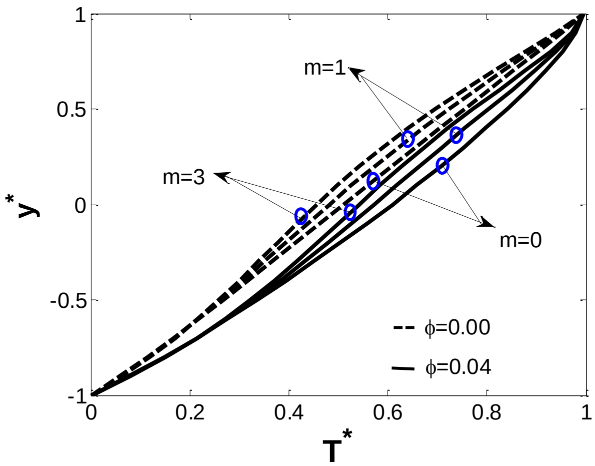

(c)

Figure 6: Effect of Hall parameter m on the velocities and temperature profiles at different values of nanoparticle volume fractions ∅.

(a) u^* Profile; (b) w^* Profile; (c) T^* Profile

5 Conclusion

In this article, the effects of nanofluid and heat transfer on Unsteady Magnetohydrodynamic flow between two infinite parallel porous plates has been numerically studied with Hall Effect in the presence of uniform suction and injection. Here, Copper as nanoparticle with water as its base fluid has been considered. Implicit finite difference method is employed to solve the equations governing the flow. The following observations are noted:

- The velocity components u^* and w^* and temperature T^* increase with the increase in the nanoparticle volume fraction $\emptyset$.
- The Cu-water nanofluid has higher values of temperature, velocity components, and steady state time compared to base fluid.
- The effect of Hartmann number H_a on the velocity components and temperature distribution for various values of nanoparticle volume fractions $\emptyset$ has been studied. By increasing H_a the x-component of the velocity u^* and temperature T^* will decrease, while the z-component of the velocity w^* will increase.

Reference

[1] Saidur, Rahman, K. Y. Leong, and Hussein A. Mohammed. "A review on applications and challenges of nanofluids." Renewable and sustainable energy reviews 15, 1646-1668, 2011.

[2] Yu, Wenhua, David M. France, Jules L. Routbort, and Stephen US Choi. "Review and comparison of nanofluid thermal conductivity and heat transfer enhancements." Heat transfer engineering 29, pp. 432-460, 2008.

[3] Choi, S. U. S., “Enhancing thermal conductivity of fluids with nanoparticles,” in Proceedings of the ASME International Mechanical Engineering Congress and Exposition, pp. 99–105, San Francisco, CA, USA, 1995.

[4] Xie, Hua-qing, Jin-chang Wang, Tong-geng Xi, and Yan Liu. "Thermal conductivity of suspensions containing nanosized SiC particles." International Journal of Thermophysics 23, pp. 571-580, 2002.

[5] Pil Jang, Seok, and Stephen US Choi. "Effects of various parameters on nanofluid thermal conductivity.", 129, pp. 617-623, 2007.

[6] Shukla, Ratnesh K., and Vijay K. Dhir. "Effect of Brownian motion on thermal conductivity of nanofluids.", 130, 042406, 2008.

[7] Abu-Nada, Eiyad. "Effects of variable viscosity and thermal conductivity of CuO-water nanofluid on heat transfer enhancement in natural convection: mathematical model and simulation.", 132, 052401, 2010.

[8] Godson, Lazarus, B. Raja, D. Mohan Lal, and S. Wongwises. "Convective heat transfer characteristics of silver-water nanofluid under laminar and turbulent flow conditions.", 4, 031001, 2012.

[9] Chandraprabu, V., G. Sankaranarayanan, S. Iniyan, and S. Suresh. "Heat transfer enhancement characteristics of Al2O3/water and CuO/water nanofluids in a tube in tube condenser fitted with an air conditioning system—an experimental comparison." Journal of Thermal Science and Engineering Applications 6, 041004, 2014.

[10] Peyghambarzadeh, S. M., S. H. Hashemabadi, M. Seifi Jamnani, and S. M. Hoseini. "Improving the cooling performance of automobile radiator with Al2O3/water nanofluid." Applied thermal engineering, 31, pp. 1833-1838, 2011.

[11] Leong, K. Y., Rahman Saidur, T. M. I. Mahlia, and Y. H. Yau. "Performance investigation of nanofluids as working fluid in a thermosyphon air preheater." International communications in heat and mass transfer, 39, pp. 523-529, 2012.

[12] Parvin, Salma, Rehena Nasrin, and M. A. Alim. "Heat transfer and entropy generation through nanofluid filled direct absorption solar collector." International Journal of Heat and Mass Transfer, 71, 386-395, 2014.

[13] Khaleduzzaman, S. S., M. R. Sohel, R. Saidur, I. M. Mahbubul, I. M. Shahrul, B. A. Akash, and J. Selvaraj. "Energy and exergy analysis of alumina–water nanofluid for an electronic liquid cooling system." International Communications in Heat and Mass Transfer , 57, pp.118-127, 2014.

[14] Abbas, W., Nabil Eldabe, and Samir Marzouk. "Soret and Dufour effects with Hall currents on peristaltic flow of Casson fluid with heat and mass transfer through non-darcy porous medium inside vertical channel." Egyptian Journal of Chemistry, 64, pp. 5215-5225, 2021.

[15] Hsiao, Kai-Long. "Stagnation electrical MHD nanofluid mixed convection with slip boundary on a stretching sheet." Applied Thermal Engineering, 98, pp. 850-861, 2016.

[16] Khan, Mair, M. Y. Malik, T. Salahuddin, and Arif Hussian. "Heat and mass transfer of Williamson nanofluid flow yield by an inclined Lorentz force over a nonlinear stretching sheet." Results in physics, 8, pp. 862-868, 2018.

[17] Pal, Dulal, and Netai Roy. "Role of Brownian motion and nonlinear thermal radiation on heat transfer of a Casson nanofluid over stretching sheet with slip velocity and non-uniform heat source/sink." Journal of Nanofluids, 8, pp. 556-568, 2019.

[18] Abbas, W., and M. M. Magdy. "Heat and mass transfer analysis of nanofluid flow based on cu, Al2O3, and TIO2 over a moving rotating plate and impact of various nanoparticle shapes." Mathematical Problems in Engineering, 2020, 9606382, 2020.

[19] Ibrahim, Wubshet, and Tezera Gizewu. "Thin film flow of tangent hyperbolic fluid with nonlinear mixed convection flow and entropy generation." Mathematical Problems in Engineering, 2021, pp.1-16, 2021.

[20] Loganathan, Karuppusamy, Nazek Alessa, and Safak Kayikci. "Heat transfer analysis of 3-D viscoelastic nanofluid flow over a convectively heated porous Riga plate with Cattaneo-Christov double flux." Frontiers in Physics, 9, 641645, 2021.

[21] Shao, Yabin, Latif Ahmad, Saleem Javed, Jawad Ahmed, Yasser Elmasry, Mowffaq Oreijah, and Kamel Guedri. "Heat and mass transfer analysis during Homann Visco-elastic slippery motion of nano-materials." International Communications in Heat and Mass Transfer, 139, 106425, 2022.

[22] Attia, Hazem Ali, Abbas, W., Mostafa AM Abdeen, and M. S. Emam. "Effect of porosity on the flow of a dusty fluid between parallel plates with heat transfer and uniform suction and injection." European journal of environmental and civil engineering, 18, pp. 241-251, 2014.

[23] Abdeen, M., and H. Attia. "Unsteady flow in a porous medium between parallel plates in the presence of uniform suction and injection with heat transfer." International Journal of Civil Engineering, 12, pp. 277-281, 2014.

[24] Umavathi, J. C., Ali J. Chamkha, M. H. Manjula, and A. Al-Mudhaf. "Magneto-convection of a two-fluid flow through a vertical channel.", 23, pp. 151–164, 2005.

[25] Kandaswamy, P., S. Malliga Sundari, and N. Nithyadevi. "Magnetoconvection in an enclosure with partially active vertical walls." International Journal of Heat and Mass Transfer ,51, pp. 1946–1954, 2008.

[26] Chamkha, Ali J., and Sameh E. Ahmed. "Unsteady MHD stagnation-point flow with heat and mass transfer for a three-dimensional porous body in the presence of heat generation/absorption and chemical reaction." Progress in Computational Fluid Dynamics, an International Journal, 11, 388-396, 2011.

[27] Nemati, H., M. Farhadi, K. Sedighi, H. R. Ashorynejad, and E. J. S. I. Fattahi. "Magnetic field effects on natural convection flow of nanofluid in a rectangular cavity using the Lattice Boltzmann model." Scientia Iranica, 19, pp. 303-310, 2012.

[28] Abdeen, M. A.M, Attia, H. A., Abbas, W., Abd El-Meged, W.. "Effectiveness of porosity on transient generalized Couette flow with Hall effect and variable properties under exponential decaying pressure gradient." Indian Journal of Physics, 87, pp. 767-775, 2013.

[29] Srinivasulu, Thadakamalla, and B. Shankar Goud. "Effect of inclined magnetic field on flow, heat and mass transfer of Williamson nanofluid over a stretching sheet." Case Studies in Thermal Engineering 23, 100819, 2021.

[30] Megahed, Ahmed M. "Improvement of heat transfer mechanism through a Maxwell fluid flow over a stretching sheet embedded in a porous medium and convectively heated." Mathematics and Computers in Simulation, 187, pp. 97-109, 2021.

[31] Biswal, Manasa M., Bharat K. Swain, Manjula Das, and Gouranga Charan Dash. "Heat and mass transfer in MHD stagnation-point flow toward an inclined stretching sheet embedded in a porous medium." Heat Transfer, 51, pp. 4837-4857, 2022.

[32] Abbas, W., and Ahmed M. Megahed. "Numerical solution for chemical reaction and viscous dissipation phenomena on non-Newtonian MHD fluid flow and heat mass transfer due to a nonuniform stretching sheet with thermal radiation." International Journal of Modern Physics C, 32, pp. 2150124, 2021.

[33] Abdelsalam, Sara I., W. Abbas, Ahmed M. Megahed, and Ahmed AM Said. "A comparative study on the rheological properties of upper convected Maxwell fluid along a permeable stretched sheet." Heliyon, 9, e22740, 2023.

[34] Gautam, Anil Kumar, Sohita Rajput, Krishnendu Bhattacharyya, Amit Kumar Pandey, Ali J. Chamkha, and Momtaz Begum. "Comparative study of two non-Newtonian fluids with bioconvective induced MHD flow in presence of multiple slips, heat source/sink and nonlinear thermal radiation." Chemical Engineering Journal Advances, 12, 100365, 2022.

[35] Abbas, W., Ahmed M. Megahed, M. A. Ibrahim, and Ahmed AM Said. "Ohmic dissipation impact on flow of Casson-Williamson fluid over a slippery surface through a porous medium." Indian Journal of Physics, 97, 4277-4283, 2023.

[36] Amer, A. M., Salim AS Al Rashdi, Nourhan I. Ghoneim, and Ahmed M. Megahed. "Tangent hyperbolic nanofluid flowing over a stretching sheet through a porous medium with the inclusion of magnetohydrodynamic and slip impact." Results in Engineering, 19, 101370, 2023.

[37] Elgendi, S. G., Abbas, W., Ahmed AM Said, Ahmed M. Megahed, and Eman Fares. "Computational Analysis of the Dissipative Casson Fluid Flow Originating from a Slippery Sheet in Porous Media." Journal of Nonlinear Mathematical Physics 31, 19, 2024.

[38] Sadiq, Naeem, Muhammad Jawad, Fareeha Khalid, Shah Jahan, and Ahmed M. Hassan. "Comparative Analysis of Non-Newtonian and Newtonian Fluid Flow with Dual Slip in the Presence of Motile Microorganisms and Nanoparticles." BioNanoScience, 2024, pp. 1-16, 2024.

[39] Attia, H. A., Abbas, W., M. Abdeen, A. M., El-Din Abdin, A.. "Effect of porosity on the flow and heat transfer between two parallel porous plates with the Hall effect and variable properties under constant pressure gradient." Blug. Chem. Commun 46, pp. 535 – 544, 2014.

[40] Khanafer, Khalil, and Kambiz Vafai. "A critical synthesis of thermophysical characteristics of nanofluids." In Nanotechnology and energy, 54, pp. 279-332, 2017.

[41] Selimefendigil, Fatih, and Hakan F. Öztop. "Numerical study of MHD mixed convection in a nanofluid filled lid driven square enclosure with a rotating cylinder." International journal of heat and mass transfer 78, pp. 741-754, 2014.

[42] He, Ji-Huan. "A coupling method of a homotopy technique and a perturbation technique for non-linear problems." International journal of non-linear mechanics, 35, pp. 37-43, 2000.

[43] Wu, Yue, and Ji-Huan He. "Homotopy perturbation method for nonlinear oscillators with coordinate dependent mass." Results Phys, 10, pp. 270-271, 2018.

[44] Abbas, W., Magdy, M. M., Abdelgaber, K. M., Abdeen, M. A.M. "Unsteady magnetohydrodynamic flow with heat and mass transfer between two parallel walls under variable magnetic field." High Temperature, 58, 284-291, 2020.

Nomenclature

B	induced magnetic field
B_0	magnetic field density
c_P	specific heat capacity
E	electric field intensity
Ec	Eckert number
Ha	Hartmann number
J	electric current density
k	thermal conductivity
m	Hall parameter
P	pressure
Pr	Prandtl number
Re	Reynolds number
S	suction parameter
t	time
t^*	dimensionless time
T	temperature
T^*	dimensionless temperature
u, w	velocity components along x, and z axes, respectively
u^*, w^*	dimensionless velocity components along x,

	and z axes, respectively
$\vec{v}$	Velocity vector
Greek symbols	
β	Hall factor
ρ	density
ρ^*	dimensionless density
$\emptyset$	nanoparticles volume fraction
σ	electric conductivity
μ	viscosity
Subscripts	
f	base fluid
nf	nanofluid
p	solid particle